THE JOURNAL OF BIOLOGICAL CHEMISTRY VOL. 282, NO. 27, pp. 19884–19893, July 6, 2007


# Singar1, a Novel RUN Domain-containing Protein, Suppresses Formation of Surplus Axons for Neuronal Polarity*◆

Received for publication, January 26, 2007, and in revised form, April 10, 2007 Published, JBC Papers in Press, April 17, 2007, DOI 10.1074/jbc.M700770200

**Tatsuya Mori‡, Tomoe Wada‡, Takahiro Suzuki‡, Yoshitsugu Kubota§, and Naoyuki Inagaki‡1**

*From the ‡Division of Signal Transduction, Nara Institute of Science and Technology, Ikoma 630-0192 and the §Department of Transfusion Medicine, Faculty of Medicine, Kagawa University, Kagawa 760-0793, Japan*

**Although neuronal functions depend on their robust polarity, the mechanisms that ensure generation and maintenance of only a single axon remain poorly understood. Using highly sensitive two-dimensional electrophoresis-based proteomics, we identified here a novel protein, single axon-related (singar)1/KIAA0871/RPIPx/RUFY3, which contains a RUN domain and is predominantly expressed in the brain. Singar1 expression became up-regulated during polarization of cultured hippocampal neurons and remained at high levels thereafter. Singar1 was diffusely localized in hippocampal neurons and moderately accumulated in growth cones of minor processes and axons. Overexpression of singar1 did not affect normal neuronal polarization but suppressed the formation of surplus axons induced by excess levels of shootin1, a recently identified protein located upstream of phosphoinositide-3-kinase and involved in neuronal polarization. Conversely, reduction of the expression of singar1 and its splicing variant singar2 by RNA interference led to an increase in the population of neurons bearing surplus axons, in a phosphoinositide-3-kinase-dependent manner. Overexpression of singar2 did not suppress the formation of surplus axons induced by shootin1. We propose that singar1 ensures the robustness of neuronal polarity by suppressing formation of surplus axons.**

Most neurons develop polarity by forming a single long axon and multiple short dendrites (1, 2). The ability of neurons to develop and maintain polarity is essential for their basic functions. The polarization processes have been extensively studied in cultured hippocampal neurons (1, 3). These cells first form several minor processes, any of which appears capable of becoming either an axon or a dendrite, during the first 12–24 h after plating (stage 2). One of the neurites then rapidly elongates to acquire axonal characteristics (stage 3), whereas the others later become dendrites (stage 4). Hippocampal neurons must use a robust internal mechanism that ensures polarization as they regenerate a single axon and multiple dendrites even when polarity is altered by axonal amputation (4, 5).

Recent studies have begun to reveal molecules involved in neuronal polarization (6–8). Localization, overexpression, and loss of function studies showed that spatially localized intracellular signals of a number of molecules, such as phosphoinositide-3-kinase (PI 3-kinase)[2] (9), phosphatidylinositol (3, 4, 5) triphosphate (10), Akt (11), glycogen synthase kinase-3$\beta$ (11–13), collapsin response mediator protein-2 (CRMP-2) (12, 14), mPar3/mPar6/atypical protein kinase C complex (9, 15), Cdc42 (15, 16), Rap1B (16), STEF/Tiam1 (15, 17), Rac (15), adenomatous polyposis coli (18), JNK (19), and DOCK7 (20) are involved in axon specification for neuronal polarity formation. As downstream events, these pathways are thought to regulate cytoskeletal networks of actin filaments (21) and microtubules (20, 22).

In contrast to the progress in defining the mechanisms of axon specification, our knowledge of how neurons generate and maintain only a single axon is limited. Reduction in the expression or activities of glycogen synthase kinase-3$\beta$, PTEN, or microtubule affinity-regulation kinase (MARK)2 in hippocampal neurons leads to formation of multiple axons (11, 12, 23), suggesting that these molecules may be involved in inhibiting the formation of surplus axons. Recently, we identified the protein shootin1, which is located upstream of PI 3-kinase and involved in neuronal polarization (24). During polarization, shootin1 accumulated in a single neurite while being depleted in its sibling neurites, through competitive transport to multiple neurites. This in turn induced formation of a single axon, leading us to propose that the depletion of shootin1 from the sibling neurites of the nascent axon by competition prevents the formation of surplus axons (24).

We describe here a novel brain-specific protein, named single axon-related (singar)1. Singar1 became up-regulated during polarization of cultured hippocampal neurons and remained at

* This work was supported in part by Grants-in-Aid for Scientific Research on Priority Areas 18016020 and 18022028 from the Ministry of Education, Culture, Sports, Science and Technology of Japan, the Japan Society for the Promotion of Science KAKENHI (Grant 18300107), and a grant from the Osaka Medical Research Foundation for Incurable Diseases. The costs of publication of this article were defrayed in part by the payment of page charges. This article must therefore be hereby marked "*advertisement*" in accordance with 18 U.S.C. Section 1734 solely to indicate this fact.

◆ This article was selected as a Paper of the Week.

[S] The on-line version of this article (available at http://www.jbc.org) contains two supplemental figures.

[1] To whom correspondence should be addressed. Tel.: 81-743-72-5441; Fax: 81-743-72-5449; E-mail: ninagaki@bs.naist.jp.

[2] The abbreviations used are: PI 3-kinase, phosphoinositide-3-kinase; 2-DE, two-dimensional electrophoresis; CMFDA, 5-chloromethylfluorescein diacetate; DIV, day *in vitro*; E, embryonic day; P, postnatal day; GST, glutathione S-transferase; MALDI-MS, matrix-assisted laser desorption/ionization mass spectrometry; MALDI-TOF MS, matrix-assisted laser desorption/ionization-time of flight mass spectrometry; MARK2, microtubule affinity-regulation kinase; RUN domain, RPIP8, UNC-14 and NESCA homology domain; RPIPx, Rap2 interacting protein X; scRNA, scramble RNA; siRNA, small interfering RNA; RNAi, RNA interference; singar, single axon-related; PTEN, phosphatase and tensin homolog; GFP, green fluorescent protein.

high levels thereafter. Reduction of singar1 expression by RNAi led to an increase in the population of neurons bearing surplus axons, as has been reported for glycogen synthase kinase-3$\beta$, PTEN, and MARK2. Furthermore, overexpression of singar1 suppressed the formation of surplus axons induced by excess amounts of shootin1, without affecting normal polarization processes. These data suggest that singar1 suppresses the formation of surplus axons, thereby contributing to the robustness of neuronal polarity.

## EXPERIMENTAL PROCEDURES

*Cultures and Metabolic Labeling*—Hippocampal neurons prepared from E18 rat embryos were seeded on coverslips coated with poly-D-lysine (Sigma) and laminin (Iwaki) and cultured in Neurobasal medium (Invitrogen) supplemented with B-27 supplement (Invitrogen) and 1 mM glutamine without glia feeder layer as described (14). For quantitative two-dimensional electrophoresis (2-DE), stage 2 and stage 3 neurons were metabolically labeled with the culture medium containing 13% of the normal levels of methionine and cysteine plus Pro-mix L-[$^{35}$S] *in vitro* cell labeling mix (containing ~70% L-[$^{35}$S]methionine and ~30% L-[$^{35}$S]cysteine, 80 $\mu$Ci/ml; GE Healthcare) for 4 h. To prepare this labeling medium, we used custom-made Neurobasal medium without methionine and cysteine (Invitrogen). HEK293T cells were cultured in Dulbecco's modified Eagle's medium supplemented with 10% fetal calf serum.

*Highly Sensitive 2-DE and Protein Identification by Mass Spectrometry*—2-DE was performed as reported previously (25), using a composite gel series comprising a total 93 × 103-cm combined gel system (26). For differential 2-DE, neurons were metabolically labeled as above, and protein spots separated by 2-DE gels were visualized by autoradiography. For protein identification, unlabeled protein samples from 2-week-old rat brains were separated by the 2-DE gel and visualized by silver staining. The protein spots corresponding to the radiolabeled ones were then excised from gels and in-gel-digested as described (27). Matrix-assisted laser desorption/ionization mass spectrometry (MALDI-MS) was performed using a Voyager™ Elite equipped with delayed extraction (Applied Biosystems). Data base searches were conducted using the Mascot program (Matrix Science) and National Center for Biotechnology Information databases.

*Cloning of Singar*—Full-length cDNAs of rat singar1 and singar2 were amplified by PCR from a rat brain cDNA library obtained from P8 Wistar rat using an RNeasy mini kit (Qiagen) with the primers 5′-GCGGATCCATGTCTGCCCTGACGCCTCCGAC-3′ and 5′-GCGGATCCCTAATGATGTTTTGGGATCAGTTTATTTG-3′. The cDNAs were then subcloned into the BamHI site of pCMV (Stratagene) -Myc, pCMV-FLAG, pCAGGS-Myc with a $\beta$-actin promoter (provided by J. Miyazaki, Osaka University, Osaka, Japan) (28), and pGEX-6P-1 (GE Healthcare) vectors. These plasmids were designed to generate the proteins fused to Myc, FLAG, and glutathione *S*-transferase (GST) tags at the N terminus. We did not use epitope tag repeats.

*Protein and Antibody Preparation*—Recombinant full-length singar1 was expressed in *Escherichia coli* BL21(DE3)codonPlus (Stratagene) as a GST fusion protein by induction with 0.1 mM isopropyl-$\beta$-D-thiogalactopyranoside at 20 °C for 4 h and purified on a glutathione-Sepharose column (GE Healthcare), after which GST was removed from singar1 by PreScission protease (GE Healthcare). Rabbit polyclonal anti-singar antibody was raised against the recombinant singar1 and affinity-purified before use.

*Immunocytochemistry, Immunoblot, and Microscopy*—Immunocytochemistry and immunoblot were performed as described (14). For immunocytochemistry, anti-Myc (monoclonal: M047-3, MBL, Nagoya, Japan), tau-1 (MAB3420, Roche Applied Science, Mannheim, Germany), anti-synaptophysin (SY38, Progen, Heidelberg, Germany), and anti-MAP-2 (HM-2, Sigma-Aldrich) antibodies were used at 1:7,000, 1:500, 1:2,500, and 1:1,000 dilution, respectively. Anti-singar antibody was used at 0.2 $\mu$g/ml. For 5-chloromethylfluorescein diacetate (CMFDA) staining, neurons were incubated with CMFDA (1:500) for 30 min before fixation. Fluorescent images of neurons were acquired using a fluorescent microscope, Axioplan2 (Carl Zeiss, Tokyo, Japan) equipped with a Plan-NEOFLUAR ×40, 0.75 NA or ×20, 0.50 NA objective, an AxioCamMRm CCD camera (Carl Zeiss), and Axiovision3 imaging software (Carl Zeiss). Line-scan analysis (1 pixel wide) was performed using MetaMorph imaging system (Universal imaging company, Downingtown, PA). Each plotted point represents a 0.32-$\mu$m average of immunoreactivity along the lines. For immunoblot, anti-Myc (polyclonal:562, MBL, Nagoya, Japan), anti-FLAG (M2: F3165, Sigma-Aldrich), and anti-$\beta$III-tubulin (TUJ-1, MMS-435P, Covance, Berkeley, CA) antibodies were used at 1:1,000, 1:5,000, and 1:2,000 dilution, respectively. Anti-singar antibody was used at 0.1 $\mu$g/ml.

*Transfection and RNAi*—Neurons were transfected with cDNA or RNA by the calcium phosphate method (14), Nucleofector (Amaxa), or Lipofectamine 2000 (Invitrogen) before or after plating. Namely, for immunoblot analysis of the effects of small interfering RNA (siRNA) on singar expression, transfection of neurons was carried out before plating using Nucleofector. For analysis of the effects of siRNA on neuronal morphology after polarization, neurons were transfected by the calcium phosphate method on day *in vitro* (DIV) 3. For the other analysis, neurons were transfected with DNA or RNA using Lipofectamine 2000 before plating. Namely, neurons suspended in Neurobasal medium containing 10% fetal calf serum were incubated with lipofectamine2000/DNA (or RNA) complex for 1.5 h. Then, they were washed by centrifugation and resuspending in Neurobasal/10% fetal calf serum and plated on coverslips. Three h after the plating, the medium was replaced by the culture medium. HEK293T cells were transfected with cDNA by the calcium phosphate method. The siRNA sequence 5′-GGCAAAAGUAGAUGCGUUA-3′ targeting rat singar1 and singar2 corresponds to nucleotides 846–864 in the coding region of singar1 (nucleotides 900–918 in the coding region of singar2). The scramble RNA (scRNA) 5′-AGCGAAGGUUGACGCUCUU-3′ encodes the same amino acid sequence as the siRNA but lacks significant sequence similarity to any gene. The RNAs were obtained from Dharmacon.

*Immunoprecipitation*—HEK293T cells were transfected with the expression plasmids and grown in 60-mm diameter culture dishes. Forty-eight h after transfection, cells were washed once

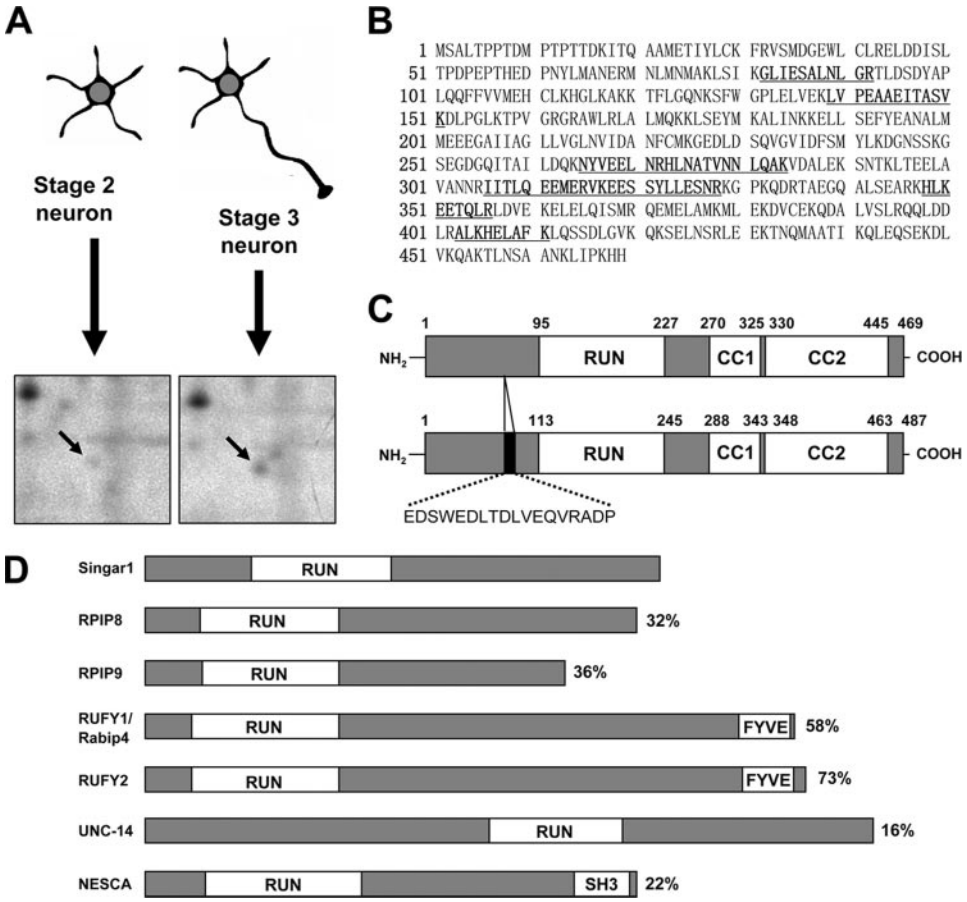


FIGURE 1. **Identification of singar1 as a protein up-regulated during polarization of rat cultured hippocampal neurons.** *A*, differential 2-DE analysis of proteins in stage 2 (cultured for 14 h) and stage 3 (cultured for 62 h) hippocampal neurons. The *arrows* indicate the protein spots of singar1 enriched in the stage 3 sample (stage 3/2 = 2.3, $n = 5$, $p < 0.01$). *B*, amino acid sequence of rat singar1. Sequences of the peptides identified by MALDI-TOF MS analysis are *underlined* and shown by *bold letters*. *C*, schematic representation of rat singar1 (*upper*) and singar2 (*lower*). Singar2 has an 18-amino-acid insertion between His-58 and Glu-59 of singar1. Singar1 and singar2 contain one RUN domain and two coiled-coil (*CC*) domains. *D*, schematic representation of singar1 and other RUN domain-containing proteins. The percentages represent the identity of the amino acid sequences of their RUN domains when compared with that of singar1.

with ice-cold PBS and harvested in the cell lysis buffer (50 mM Tris-HCl, pH 7.4, 150 mM NaCl, 2.5 mM $MgCl_2$, 2 mM EGTA, 1 mM dithiothreitol, 1 mM $Na_3VO_4$, 10 mM NaF, 0.5% Nonidet P-40, 2 mM phenylmethylsulfonyl fluoride). After incubation on ice for 30 min, the extracts were then centrifuged at 100,000 × *g* for 30 min at 4 °C. The supernatant were incubated with 1.5 μg of anti-FLAG antibodies, and immunocomplexes were precipitated with protein G-Sepharose 4B. After three times of washing with the cell lysis buffer, the beads were boiled in the SDS sample buffer and applied to immunoblot analysis.

*Materials*—Calyculin A, λ-phosphatase, CMFDA, rhodamine phalloidin, and LY294002 were obtained from WAKO (Osaka, Japan), New England Biolabs (Hitchin, UK), Molecular Probes (Eugene, OR), Molecular Probes, and Calbiochem, respectively. cDNA encoding Myr-PI 3-K p110 was from Upstate Biotechnology. cDNA encoding p85 subunit of PI 3-kinase was amplified by PCR from a rat brain cDNA library obtained as described above.

*Statistics*—In the statistical analysis for Fig. 4*A*, the neurons with one long neurite longer than 100 μm and over twice as long as the other neurites were counted as stage 3 neurons (these cells do not include neurons with multiple axons). Significance was determined by the unpaired Student's *t* test.

## RESULTS

*Identification of Singar1 by a Proteome Screening of Stage 2 and Stage 3 Hippocampal Neurons*—To identify proteins involved in neuronal polarity formation, we previously performed proteome analysis of cultured rat hippocampal neurons using a 93 × 103-cm large gel 2-DE (26). We screened about 6,200 protein spots on 2-DE gels and detected 277 that were consistently up-regulated during the transition between stages 2 and 3 (24). Tryptic digestion and mass spectrometry of one of them, located at a molecular mass of 55 kDa and pI = 5.2 in gels (Fig. 1*A*), identified six peptides whose sequences corresponded to human (BC051716), rat (EF577045), and mouse (BC049127) cDNA sequences of KIAA0871/RUFY3/Rap2-interacting protein X (RPIPx) in genome databases (Fig. 1*B* and supplemental Fig. 1). Rat, human, and mouse KIAA0871/RUFY3/RPIPx encode proteins of 469 amino acids and predicted molecular masses of 52.9, 52.9, and 53.0 kDa, respectively. Domain searching revealed that KIAA0871/RUFY3/RPIPx contains one RUN (RPIP8, UNC-14, and NESCA) domain (29) and two coiled-coil domains (Fig. 1*C*). Recently, the crystal structure of its RUN domain was reported (30). We designated it singar1, together with Dr. Osamu Ohara (Kazusa DNA Research Institute), who initially reported its full cDNA sequence as KIAA0871 (AB020678) and Dr. Takahiro Nagase (Kazusa DNA Research Institute). It shows homology to RUN domain-containing proteins, such as RPIP8, RPIP9, RUFY1/Rabip4, RUFY2, UNC-14, and NESCA (Fig. 1*D*). Data base searches also identified *Pan troglodytes*, *Macaca mulatta*, *Bos taurus, Canis familiari,* and *Gallus gallus* orthologs of singar1, and partial open reading frames in *Xenopus laevis*, *Danio rerio*, *Fugu rubripes*, and *Drosophila*. In addition, a splicing variant of 487 amino acids was identified in rat (EF538802) and mouse (BC058259) cDNAs and termed singar2 (Fig. 1*C* and supplemental Fig. 1).

*Singar1 and Singar2 Are Predominantly Expressed in the Brain and Up-regulated during Polarization*—We raised an antibody against recombinant singar1 to investigate its tissue and intracellular distribution. The antibody recognized three

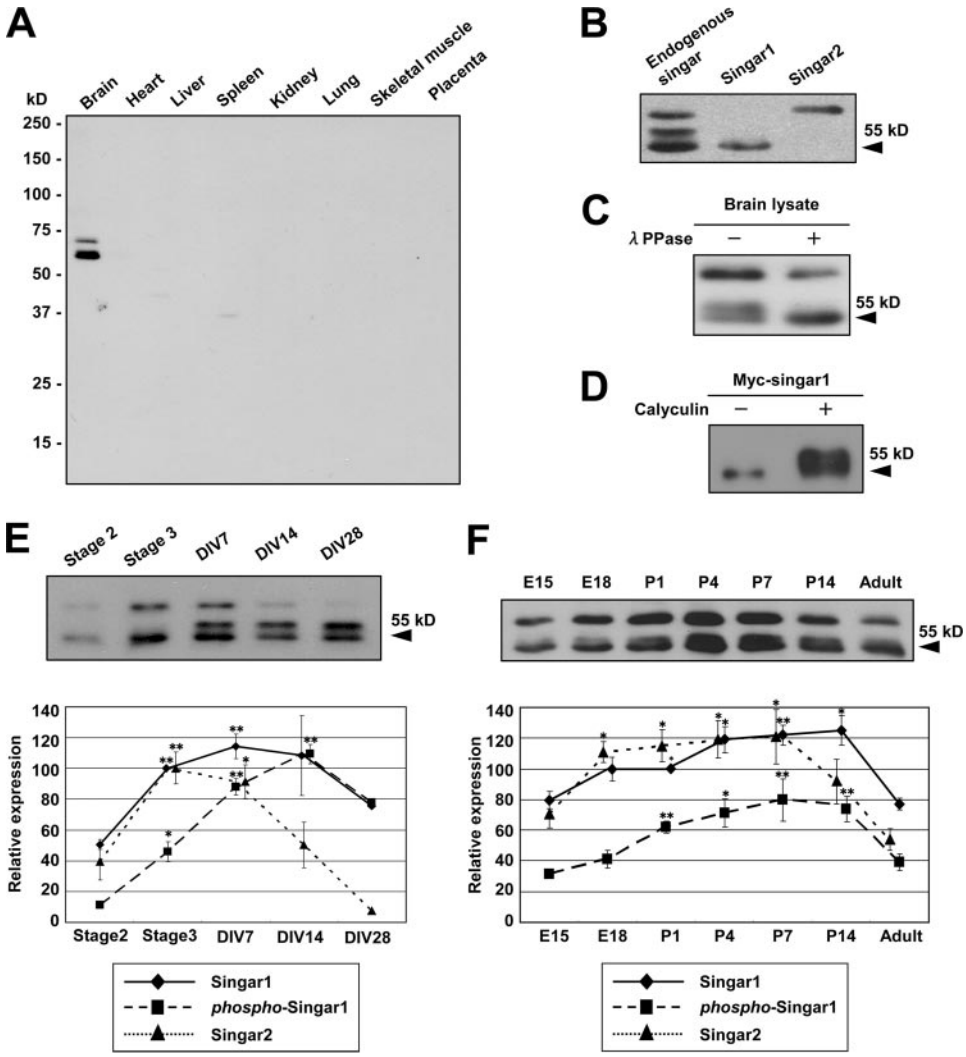


FIGURE 2. **Expressions of singar1 and singar2.** *A*, immunoblot analysis of singar in adult rat tissues. *B*, immunoblot analysis of singar in adult brain and singar1 and singar2 exogenously expressed in HEK293T cells. *C*, protein lysates from P5 rat brain were treated with 4 units/$\mu$l of λ-phosphatase for 30 min at room temperature and applied to immunoblot analysis with anti-singar antibody. *D*, HEK293T cells expressing Myc-singar1 were treated with 100 nM calyculin A or $Me_2SO$ for 20 min at 37 °C. The cells were collected, and the extracted proteins were applied to immunoblot analysis with anti-Myc antibody. *E* and *F*, immunoblot analysis of singar in rat cultured hippocampal neurons (*E*, 3 $\mu$g of proteins were loaded) and in rat brains (*F*, 5 $\mu$g of proteins were loaded) at various developmental stages. The densities of singar immunoreactivity were measured by densitometer and expressed as the percentage of the densities of singar1 in stage 3 (*E*) and on P1 (*F*), respectively. Values are S.E. for four independent experiments except DIV28 ($n = 2$) (*, $p < 0.05$; **, $p < 0.01$).

bands at 55, 60, and ~56 kDa in immunoblots of rat brain (Fig. 2*A*). The lower band corresponds to the apparent $M_r$ of recombinant singar1, whereas the upper band corresponds to that of recombinant singar2 (Fig. 2*B*), suggesting that the two splicing variants are expressed in the brain. Treatment of brain lysate with λ-phosphatase led to disappearance of the middle 56-kDa band and increase in the intensity of the lower band (Fig. 2*C*), whereas treatment of HEK293T cells expressing exogenous singar1 with the phosphatase inhibitor calyculin A increased the intensity of the middle band (Fig. 2*D*). Therefore, we concluded that the middle band corresponds to the phosphorylated form of singar1. The three bands were not detected in various peripheral tissues (Fig. 2*A*), suggesting that singar1 and singar2 are predominantly expressed in the brain. Consistent with the 2-DE data for the metabolically labeled protein (Fig. 1*A*), the level of singar1 expression increased remarkably during the transition from stage 2 to stage 3 in cultured hippocampal neurons and remained high until DIV28 (Fig. 2*E*). Consistently, expression of singar1 in rat brain was relatively low on embryonic day 15 (E15), peaked around postnatal day 4 (P4), and decreased in the adult brain (Fig. 2*F*). Similar expression patterns were observed for singar2 and phosphorylated singar1 in general, except that the expression of singar2 in hippocampal neurons returned to a low level at DIV14 and up-regulation of phosphorylated singar1 was relatively slow in the cultured neurons and brain (Fig. 2, *E* and *F*).

*Singar1 and Singar2 Accumulates in Growth Cones of Minor Processes and Axons*—Next, we examined the localization of singar in cultured hippocampal neurons. Immunocytochemical analysis showed a diffuse staining of endogenous singar in stage 2, stage 3, and stage 4 neurons (Fig. 3, *A*–*C*). In stage 2, singar immunoreactivity showed a moderate accumulation in growth cones of minor processes (*arrowheads*); 52% of growth cones showed accumulation ($n = 120$ growth cones). In stage 3, singar accumulated in growth cones of axons in addition to those of minor processes (Fig. 3*B*, *arrows* and *arrowheads*); 77% of axonal growth cones showed accumulation ($n = 56$ growth cones), whereas 52% of minor process growth cones showed accumulation ($n = 83$ growth cones). In stage 4, singar accumulated in growth cones of axons (Fig. 3*C*); 31% of axonal growth cones showed accumulation ($n = 55$ growth cones). Singar immunoreactivity was also localized in dendrites but did not show accumulation there (Fig. 3*C*). We used a green volume marker, CMFDA, as an internal standard to measure relative concentration of singar (singar immunoreactivity/CMFDA staining) (24). The relative concentrations of singar in growth cones of minor processes and axons were 2.3 ± 0.2 times ($n = 15$ growth cones) and 2.9 ± 0.2 times ($n = 15$ growth cones) higher than that in cell bodies, respectively (Fig. 3*B*). In growth cones, singar immunoreactivity was preferentially localized in F-actin-enriched filopodia and lamellipodia (Fig. 3*D*). As the anti-singar antibody recognized both singar1 and singar2, we also examined the localization of Myc-tagged singar1 and singar2 (Myc-singar1 and Myc-singar2) exogenously expressed in hippocampal neurons. Localizations of Myc-singar1 and Myc-singar2 were essentially similar to that

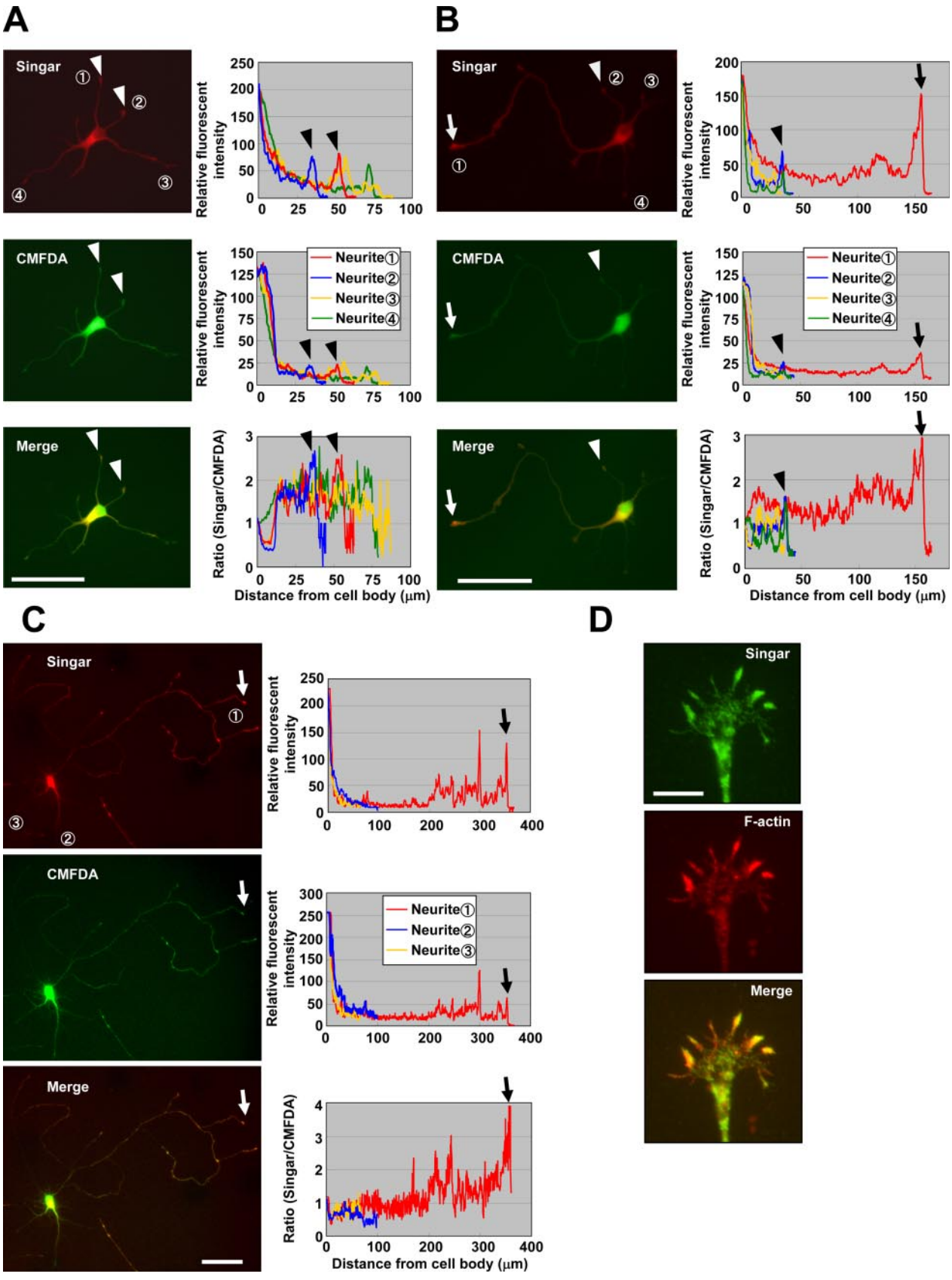


FIGURE 3. **Localization of singar in rat cultured hippocampal neurons.** *A–C*, immunofluorescent localization of singar in stage 2 (*A*), stage 3 (*B*), and stage 4 (*C*) hippocampal neurons. Neurons were double-stained by anti-singar antibody (*red*) and a volume marker CMFDA (*green*). Quantitative profiles show the relative fluorescent intensities of singar and CMFDA and relative concentration of singar (singar immunoreactivity/CMFDA staining). *Arrows* and *arrowheads* denote axonal and minor process growth cones, respectively. *Bars*, 50 μm. *D*, localization of singar in an axonal growth cone of a stage 3 hippocampal neuron. The stage 3 neuron was double-stained by anti-singar antibody (*green*) and rhodamine phalloidin (*red*). *Bar*, 10 μm.

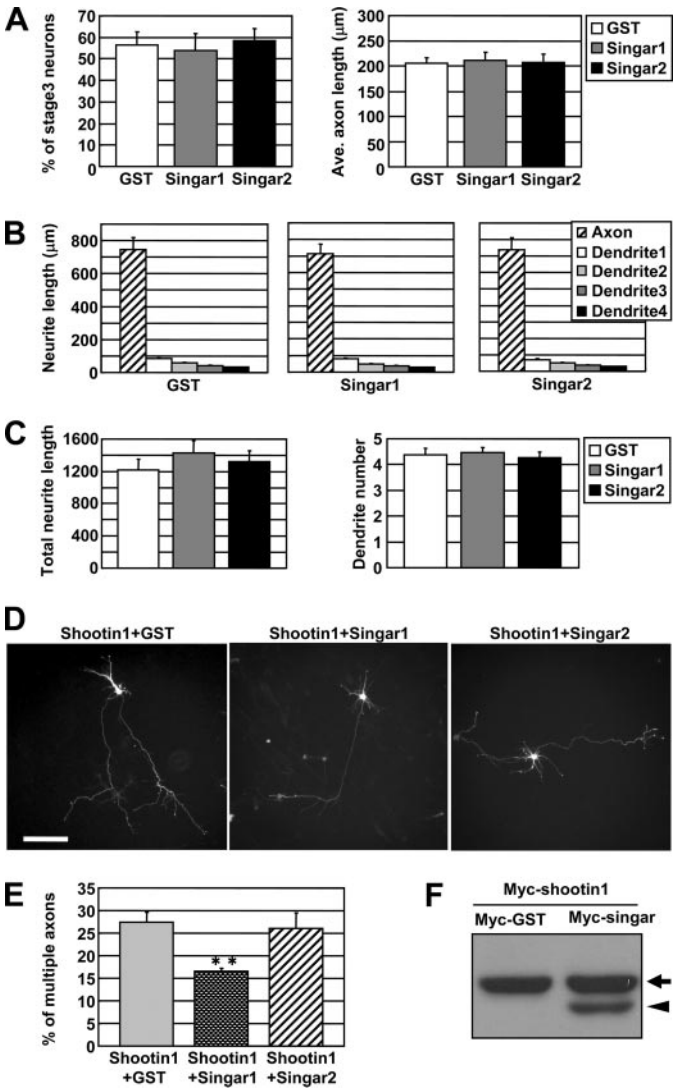


FIGURE 4. **Effect of the overexpression of singar1 and singar2 on polarization of hippocampal neurons.** *A*, the percentage (*left*) and axon length (*right*) of stage 3 neurons overexpressing Myc-GST, Myc-singar1, or Myc-singar2 at 62 h in culture. Neurons overexpressing Myc-GST, Myc-singar1, or Myc-singar2 were fixed at 62 h in culture and immunostained by anti-Myc antibody. The neurons that had one long neurite longer than 100 $\mu$m and over twice as long as the other neurites were counted as stage 3 neurons. A total of 216 neurons for GST, 239 neurons for singar1, and 289 neurons for singar2, respectively, was examined in three independent experiments. *Error bars* indicate ± S.E. *B*, axon and dendrite length of neurons overexpressing Myc-GST, Myc-singar1, or Myc-singar2 on DIV6. Neurons overexpressing Myc-GST, Myc-singar1, or Myc-singar2 were fixed on DIV6 and immunostained by anti-Myc antibody. A total of 42 neurons for GST, 42 neurons for singar1, and 40 neurons for singar2, respectively, was examined in three independent experiments. *Error bars* indicate ± S.E. *C*, total neurite length (*left*) and the number of dendrites (*right*) of neurons overexpressing Myc-GST, Myc-singar1, or Myc-singar2 on DIV6. A total of 42 neurons for GST, 42 neurons for singar1, and 40 neurons for singar2, respectively, was examined in three independent experiments. *Error bars* indicate ± S.E. *D*, neurons overexpressing Myc-shootin1 together with Myc-GST, Myc-singar1, or Myc-singar2 on DIV6. Neuron were fixed and immunostained by anti-Myc antibody. *Bar*, 50 $\mu$m. *E*, the percentage of neurons with multiple axons overexpressing Myc-shootin1 together with Myc-GST, Myc-singar1, or Myc-singar2. A total of 498 neurons for GST, 493 neurons for singar1, and 455 neurons for singar2, respectively, was examined in four independent experiments. *Error bars* indicate ± S.D. (**, $p < 0.01$). *F*, immunoblot analysis of the Myc-shootin1 expression in DIV6 neurons overexpressing Myc-shootin1 together with Myc-GST or Myc-singar1. The *arrow* indicates Myc-shootin1, and the *arrowhead* indicates Myc-singar1.

of the endogenous singar immunoreactivity (supplemental Fig. 2, *A* and *B*).

*Overexpression of Singar1 Suppresses the Formation of Surplus Axons Induced by Excess Levels of Shootin1, without Affecting Normal Polarization Processes*—To analyze the functions of singar1 and singar2 in neuronal polarization, we overexpressed Myc-tagged singar1 and singar2 in hippocampal neurons under the $\beta$-actin promoter. Neurons were transfected with cDNAs before plating, and the percentage of polarized neurons was counted at 62 h in culture. Fifty-three ± 7.8% of neurons overexpressing Myc-singar1 ($n$ = three independent cultures, 239 neurons examined) and 58 ± 5.6% of neurons overexpressing Myc-singar2 ($n$ = three independent cultures, 289 neurons examined) polarized, as in the case of control neurons with overexpressed Myc-GST (56 ± 5.8%, $n$ = three independent cultures, 216 neurons examined) (Fig. 4*A*). Axons of similar lengths were formed from neurons with overexpressed Myc-singar1, Myc-singar2, and Myc-GST (Fig. 4*A*). We further cultured the neurons with overexpressed Myc-singar1, Myc-singar2, and Myc-GST until DIV6. We did not find differences in either the length or the number of axons and dendrites among these neurons (Fig. 4, *B* and *C*). Thus, we conclude that overexpression of singar1 or singar2 does not affect normal polarization processes.

Recently, we identified the protein shootin1, which is located at an upstream position in polarity signals involving PI 3-kinase (24). Overexpression of shootin1 in hippocampal neurons leads to formation of surplus axons. Surprisingly, co-transfection of singar1 led to a reduction in the percentage of neurons with surplus axons induced by shootin1 overexpression ($n$ = four independent cultures, 493 neurons examined; $p < 0.01$, when compared with control neurons overexpressing Myc-GST) (Fig. 4, *D* and *E*). On the other hand, overexpression of singar2 did not suppress the formation of surplus axons induced by shootin1 ($n$ = four independent cultures, 455 neurons examined). Immunoblot analysis showed that overexpression of singar1 did not suppress the expression of shootin1 (Fig. 4*F*), thereby ruling out the possibility that the reduction in the percentage of neurons with surplus axons is caused by a decrease in the level of overexpressed shootin1.

*Reduction of Singar Expression by RNAi Leads to an Increase in the Population of Neurons Bearing Surplus Axons*—To further analyze the roles of singar in neuronal polarization, we reduced singar expression using an siRNA. Transfection of hippocampal neurons with an siRNA directed against singar before plating resulted in a significant decrease in the levels of endogenous singar1 and singar2 when compared with those seen after transfection with the corresponding scRNA (Fig. 5*A*). Suppression of singar in hippocampal neurons by the siRNA was also confirmed immunocytochemically (Fig. 5*B*, *arrowheads*). Transfection of neurons with the siRNA led to a 67% reduction in singar immunoreactivity when compared with the level seen after transfection with the scRNA (28 neurons examined). Remarkably, 15 ± 2.1% ($n$ = three independent cultures, 150 neurons examined; $p <$ 0.01, when compared with scRNA) of the neurons bore more

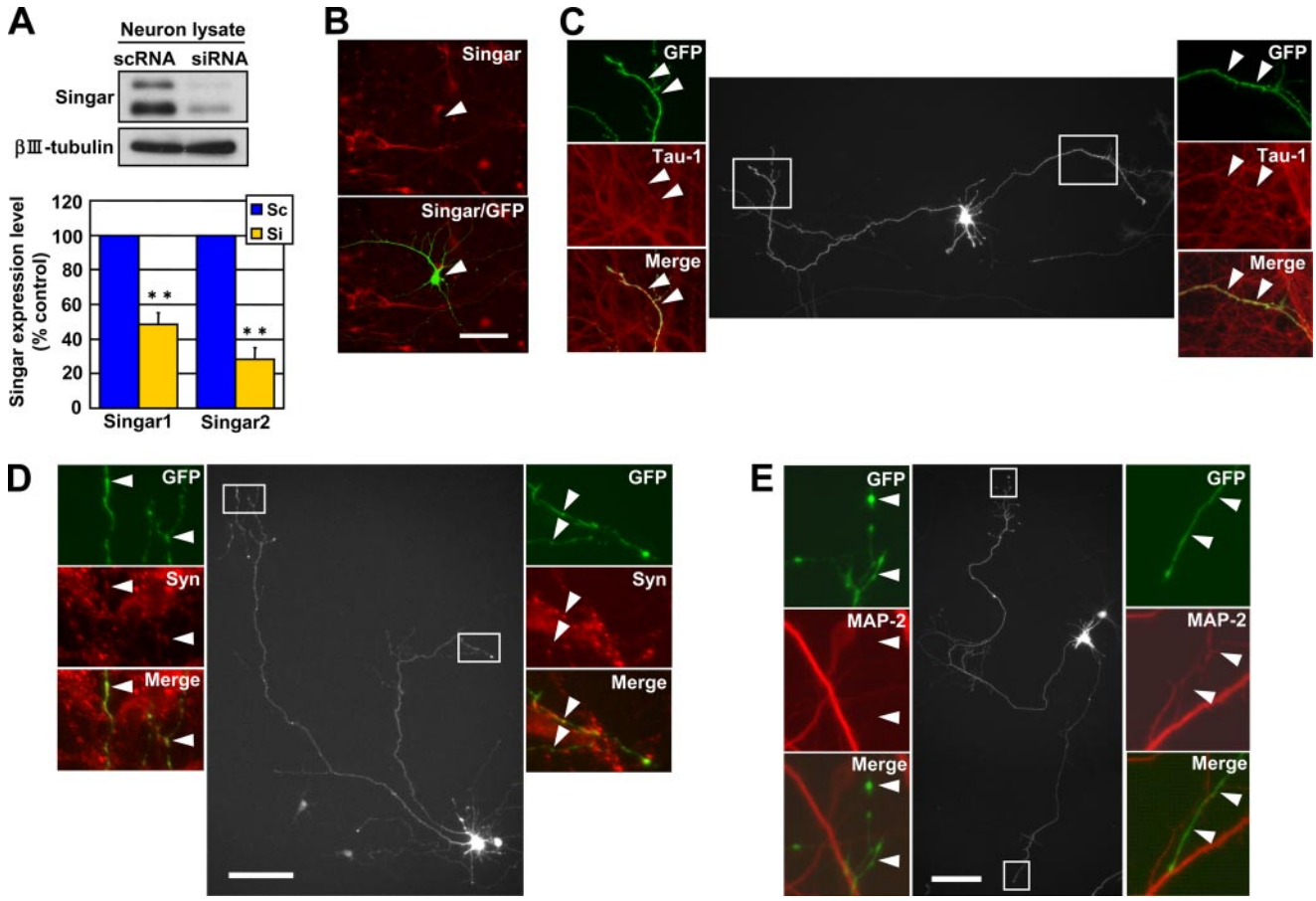


FIGURE 5. **Suppression of singar expression by RNAi induces formation of surplus axons.** *A*, suppression of singar expression in hippocampal neurons by siRNA. Proteins (3 $\mu$g) extracted from DIV3 neurons transfected with scRNA (as control) or siRNA were applied to SDS-PAGE, and the amount of singar in each sample was examined by immunoblot with anti-singar antibody. A statistical analysis of the density of the immunoreactive bands is shown below ($n = 3$; **, $p < 0.01$). *Error bars* indicate ± S.D. *B*, singar immunoreactivity of neurons transfected with siRNA. Neurons co-transfected with siRNA and pEGFP were fixed on DIV6 and immunostained by anti-singar antibody (*red*). The *arrowhead* indicates a GFP-positive (*green*) transfected neuron. *C–E*, morphological analysis of singar RNAi-treated neurons. Neurons co-transfected with siRNA and pEGFP were fixed on DIV6 and visualized by the fluorescence of GFP. The neurons were also immunostained by tau1 (*C*), anti-synaptophysin (*D*), or anti-MAP2 (*E*) antibody. *Arrowheads* indicate axons labeled by tau-1 (*C*) and anti-synaptophysin (*D*) but not by anti-MAP2 (*E*) antibody. *Bars*, 50 $\mu$m.

than one (two or three) axons that were immunostained by axon-specific markers tau-1 (Fig. 5*C*) and anti-synaptophysin (Fig. 5*D*) antibodies but were immunonegative for a dendrite-specific marker anti-MAP2 antibody (Fig. 5*E*), on DIV6 (Fig. 6*A*). In contrast, only 5.9 ± 0.2% ($n$ = three independent cultures, 159 neurons examined) of control neurons transfected with scRNA formed supernumerary axons. We also quantified the length and number of the neurites. Neurites labeled by axonal markers were markedly longer than dendrites (Fig. 6*B*). The sum of the lengths of neurites in the neurons bearing surplus axons was longer than that in control neurons (Fig. 6*C*). However, total neurite number in the neurons with surplus axons was similar to that of control neurons (Fig. 6*D*). Therefore, reduction of singar expression appears to induce surplus axons without changing the total number of neurites. In addition, reduction of singar expression enhanced the formation of surplus axons induced by shootin1 overexpression (Fig. 6*E*). Thirty-three ± 4% ($n$ = three independent cultures, 426 neurons examined; $p < 0.004$, when compared with scRNA) of the neurons co-transfected with shootin1 and siRNA bore multiple axons. In contrast, 24 ± 6% ($n$ = three independent cultures, 362 neurons examined) of control neurons co-transfected with shootin1 and scRNA formed supernumerary axons.

We next reduced singar expression after hippocampal neurons established polarity. Neurons were cultured until DIV3 to polarize (stage 3), after which they were transfected with the siRNA or scRNA, and their morphology was examined on DIV6. Twenty ± 2.1% ($n$ = three independent cultures, 131 neurons examined; $p < 0.01$, when compared with scRNA) of the neurons bore multiple axons that were immunostained by tau-1 (Fig. 7*A*) and anti-synaptophysin (data not shown) antibodies but were immunonegative for anti-MAP2 antibody (data not shown) (Fig. 7*B*). In contrast, 6.3 ± 0.3% ($n$ = three independent cultures, 160 neurons examined) of control neurons transfected with siRNA formed supernumerary axons. Together with the data of singar1 up-regulation and overexpression, these results suggest that singar plays an important role in suppressing the formation of unnecessary axons for neuronal polarity.

*Singar1 Binds to PI 3-kinase and Singar RNAi-induced Surplus Axon Formation Is Suppressed by the PI 3-kinase Inhibitor LY294002*—Shootin1 is reported to induce axons through the PI 3-kinase pathway (24), and shootin1-induced

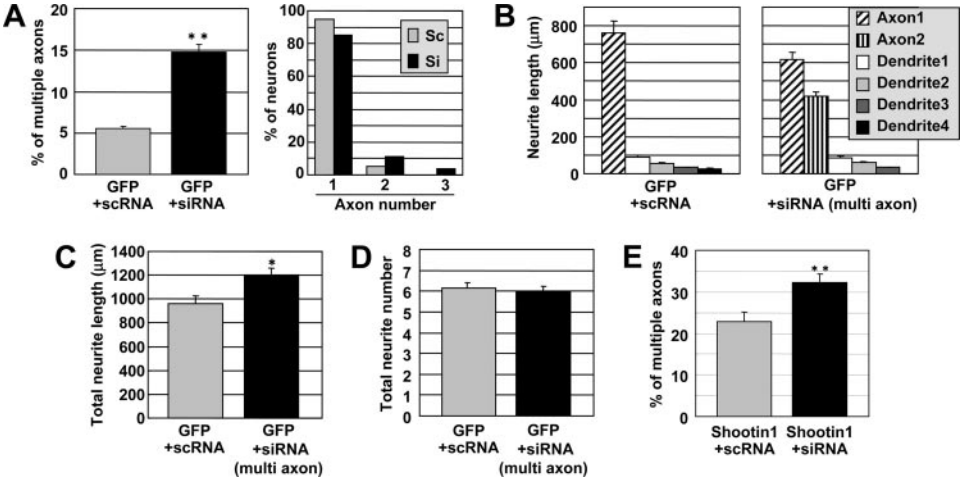


FIGURE 6. **Quantitative analysis of the morphology of neurons with suppressed expression of singar.** *A*, the percentage of singar RNAi-treated neurons (DIV6) with multiple axons and the percentage of neurons bearing one, two, or three axons. A total of 159 neurons transfected with scRNA and 150 neurons transfected with siRNA, respectively, was examined in three independent experiments. Axons were identified by tau-1 staining. *Error bars* indicate ± S.D. (**, $p < 0.01$). *B*, axon and dendrite length of singar RNAi-treated neurons (DIV6) with multiple axons. A total of 33 neurons transfected with scRNA and 28 neurons transfected with siRNA, respectively, was examined. *Error bars* indicate ± S.E. *C* and *D*, total neurite length (*C*) and total neurite number (*D*) of scRNA-treated neurons and singar RNAi-treated neurons with multiple axons (DIV6). A total of 36 neurons transfected with scRNA and 26 neurons transfected with siRNA, respectively, was examined. For *C*, *error bars* indicate ± S.E. (*, $p < 0.02$). For *D*, *error bars* indicate ± S.D. *E*, effect of singar RNAi on the formation of surplus axons induced by overexpression of shootin1. Neurons co-transfected with Myc-shootin1 and scRNA or Myc-shootin1 and siRNA were fixed on DIV6 and analyzed. A total of 362 neurons for Myc-shootin1 with scRNA and 426 neurons for Myc-shootin1 with siRNA, respectively, was examined in three independent experiments. Axons were identified by tau-1 staining. *Error bars* indicate ± S.E. (**, $p < 0.01$).

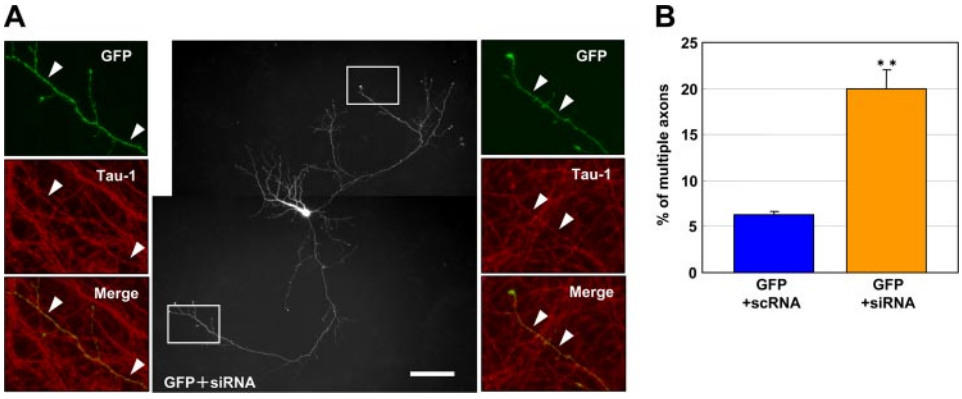


FIGURE 7. **Suppression of singar expression after polarization induces formation of surplus axons.** *A*, hippocampal neurons were co-transfected with scRNA and pEGFP or with siRNA and pEGFP on DIV3. After 3 days in culture, neurons were fixed and visualized by the fluorescence of GFP. The neurons were also immunostained by tau1 antibody (*red*). *Bar*, 50 μm. *B*, the percentage of neurons with multiple axons. A total of 160 neurons transfected with scRNA and 131 neurons transfected with siRNA, respectively, in three independent experiments was examined. *Error bars* indicate ± S.D. (**, $p < 0.01$).

multiple axon formation was suppressed by singar1 overexpression (Fig. 4, *D* and *E*) and enhanced by singar RNAi (Fig. 6*E*). We finally examined whether singar1 interacts with the PI 3-kinase pathway. Singar1 was coexpressed with the p85 or p110α subunit of PI 3-kinase in HEK293 cells. When singar1 was immunoprecipitated, co-precipitation of the p85 and p110α subunits was detected (Fig. 8, *A* and *B*). Singar1 was also reciprocally co-immunoprecipitated with the p85 and p110α subunits, indicating that it associates with PI 3-kinase. We further examined whether the formation of surplus axons induced by reduction of singar levels depends on PI 3 kinase activity. Inhibition of PI 3-kinase activity by 20 μM LY294002 led to a reduction in the percentage of neurons with multiple axons induced by singar RNAi (Fig. 8*C*). Overexpression of constitutively active PI 3-kinase (Myr-PI 3-K p110) is reported to induce formation of multiple axons as in the case of shootin1 overexpression (24, 31). Interestingly, in contrast to the case of shootin1 overexpression (Fig. 6*E*), singar RNAi did not affect the formation of surplus axons induced by the active PI 3-kinase (Fig. 8*D*). These results indicate that formation of surplus axons induced by the reduction of singar is dependent on PI 3-kinase activity, but surplus axon formation induced by the active PI 3-kinase is not influenced by singar reduction.

## DISCUSSION

Using highly sensitive 2-DE-based proteomics, we have identified here a novel protein, singar1, which is predominantly expressed in the brain. Singar1 expression became up-regulated during polarization of cultured hippocampal neurons and remained at high levels thereafter. Overexpression of singar1 suppressed the formation of surplus axons induced by excess levels of shootin1. Conversely, repression of singar by RNAi led to an increase in the population of neurons bearing surplus axons. Reduction of singar expression also enhanced the formation of surplus axons induced by shootin1 overexpression. Our siRNA decreased the levels of both singar1 and singar2, and we could not design specific siRNAs for singar1 or singar2. However, since only singar1 showed the activity to suppress the formation of surplus axons induced by shootin1, we consider that the effect of RNAi results from the reduction of singar1, not singar2. Interestingly, singar2 was found in rat and mouse databases but not in human databases. The functions of singar2 in rat and mouse hippocampal neurons remain unknown. Taken together, the present results suggest that singar1 plays an important role in suppressing formation of surplus axons.

Recent studies have reported that reduction in the expression or activities of glycogen synthase kinase-3β, PTEN, or MARK2 in hippocampal neurons leads to formation of multiple axons (11, 12, 23). Although these phenotypes are sim-

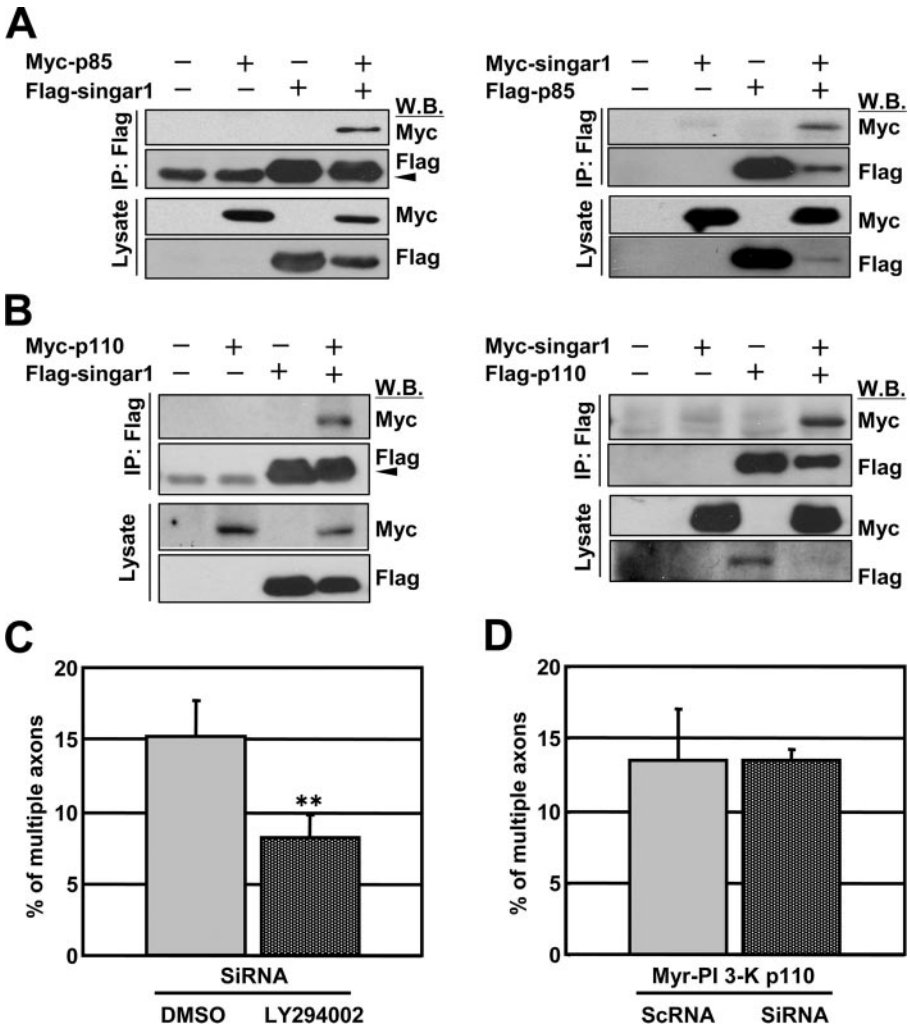


FIGURE 8. **Formation of surplus axons induced by singar RNAi depends on PI 3-kinase activity.** *A*, co-immunoprecipitation of singar1 and the p85 subunit of PI 3-kinase in HEK293T cells. The cell lysate from HEK293T cells transfected with Myc-p85 and FLAG-singar1 (*left*) or transfected with Myc-singar1 and FLAG-p85 were incubated with anti-FLAG antibody. The immunoprecipitates were analyzed by immunoblot (*W.B.*) with anti-Myc and anti-FLAG antibodies. The *arrowhead* indicates the IgG heavy chain. *B*, co-immunoprecipitation of singar1 and the p110 subunit of PI 3-kinase in HEK293T cells. The cell lysate from HEK293T cells transfected with Myc-p110 and FLAG-singar1 (*left*) or transfected with Myc-singar1 and FLAG-p110 were incubated with anti-FLAG antibody. The immunoprecipitates were analyzed by immunoblot with anti-Myc and anti-FLAG antibodies. The *arrowhead* indicates the IgG heavy chain. *C*, effect of LY294002 on the formation of surplus axons induced by singar RNAi. Neurons co-transfected with siRNA and pEGFP were treated with 20 $\mu$M LY294002 or $Me_2SO$ (*DMSO*) on DIV1 and cultured until DIV6. The percentage of neurons with surplus axons is shown. A total of 208 neurons for $Me_2SO$ and 214 neurons for LY294002, respectively, was examined in three independent experiments. *Error bars* indicate ± S.D. (**, $p < 0.01$). *D*, effect of singar RNAi on the formation of the surplus axons induced by overexpression of Myr-PI 3-K p110. The neurons co-transfected with Myr-PI 3-K p110 and scRNA or with Myr-PI 3-K p110 and siRNA were fixed on DIV6. A total of 175 neurons transfected with Myr-PI 3-K p110 and scRNA and 207 neurons transfected with Myr-PI 3-K p110 and siRNA, respectively, was examined in three independent experiments. *Error bars* indicate ± S.D.

ilar to that of singar RNAi, their overexpression phenotypes differ. Overexpression of constitutively active and wild-type glycogen synthase kinase-3$\beta$ (11, 12), wild-type PTEN (11), and wild-type MARK2 (23) inhibited formation and elongation of axons during polarization processes. On the other hand, singar1 overexpression did not affect the formation or elongation of axons during normal polarization processes but inhibited the formation of surplus axons induced by shoootin1 overexpression. Thus, our results suggest that singar1 may ensure the robustness of neuronal polarity by specifically suppressing formation of surplus axons. As observed *in vitro*, small populations of neurons with surplus axons are reported in the central nervous system (32–34). It remains to be determined whether singar1 suppresses the formation of surplus axons *in situ*.

At present, the mechanisms by which singar1 inhibits the formation of surplus axons are unclear. Singar1 overexpression inhibited the formation of surplus axons induced by shootin1 overexpression, whereas singar1 RNAi enhanced it. During polarization, shootin1 accumulates in a single neurite, whereas being depleted in its sibling neurites (24). This in turn generates polarized activity of PI 3-kinase (24), which is essential for neuronal polarization (6, 9). On the other hand, shootin1 overexpression induces its own ectopic accumulation in the growth cones of minor processes, which in turn results in ectopic accumulation of PI 3-kinase activity there and formation of surplus axons (24). In the case of singar1, a substantial amount of singar1 was observed in minor processes and dendrites. In addition, reduction of singar expression by RNAi led to an increase in the population of neurons bearing surplus axons in a PI 3-kinase-dependent manner. Therefore, singar1 in minor processes and dendrites may inhibit the formation of surplus axons by acting upstream of PI 3-kinase. Probably, locally distributed shootin1 and globally distributed singar1 may coordinately contribute to the maintenance of a single axon in neurons. In addition, singar1 accumulated in the axon might not be involved in suppressing axon formation. Interestingly, the present study detected a phosphorylated form of singar1, raising the possibility that the functions of singar 1 may be altered by protein kinases.

In conclusion, the present study has identified a novel RUN domain-containing protein singar1. Our results suggest that singar1 may ensure the robustness of neuronal polarity by suppressing formation of surplus axons without affecting normal neuronal polarization. The *in situ* functions of singar1 and the molecular details of how singar1 inhibits the formation of surplus axons remain important issues for future investigation.

*Acknowledgments—We thank Dr. Goro Eguchi and the advisors of Recognition and Formation, PRESTO for suggestions; Dr. Hiroshi Itoh for discussion; Dr. Ian Smith for reviewing the manuscript; Drs. Takahiro Nagase and Osamu Ohara for providing the cDNA encoding human KIAA0871; and Kumiko Motegi for secretarial assistance.*

## REFERENCES


1. Craig, A. M., and Banker, G. (1994) *Annu. Rev. Neurosci.* **17,** 267–310
2. Winckler, B., and Mellman, I. (1999) *Neuron* **23,** 637–640
3. Dotti, C. G., Sullivan, C. A., and Banker, G. A. (1988) *J. Neurosci.* **8,** 1454–1468
4. Dotti, C. G., and Banker, G. A. (1987) *Nature* **330,** 254–256
5. Goslin, K., and Banker, G. (1989) *J. Cell Biol.* **108,** 1507–1516
6. Arimura, N., and Kaibuchi, K. (2005) *Neuron* **48,** 881–884
7. Jiang, H., and Rao, Y. (2005) *Nat. Neurosci.* **8,** 544–546
8. Wiggin, G. R., Fawcett, J. P., and Pawson, T. (2005) *Dev. Cell* **8,** 803–816
9. Shi, S. H., Jan, L. Y., and Jan, Y. N. (2003) *Cell* **112,** 63–75
10. Menager, C., Arimura, N., Fukata, Y., and Kaibuchi, K. (2004) *J. Neurochem.* **89,** 109–118
11. Jiang, H., Guo, W., Liang, X., and Rao, Y. (2005) *Cell* **120,** 123–135
12. Yoshimura, T., Kawano, Y., Arimura, N., Kawabata, S., Kikuchi, A., and Kaibuchi, K. (2005) *Cell* **120,** 137–149
13. Gartner, A., Huang, X., and Hall, A. (2006) *J. Cell Sci.* **119,** 3927–3934
14. Inagaki, N., Chihara, K., Arimura, N., Menager, C., Kawano, Y., Matsuo, N., Nishimura, T., Amano, M., and Kaibuchi, K. (2001) *Nat. Neurosci.* **4,** 781–782
15. Nishimura, T., Yamaguchi, T., Kato, K., Yoshizawa, M., Nabeshima, Y., Ohno, S., Hoshino, M., and Kaibuchi, K. (2005) *Nat. Cell Biol.* **7,** 270–277
16. Schwamborn, J. C., and Puschel, A. W. (2004) *Nat. Neurosci.* **7,** 923–929
17. Kunda, P., Paglini, G., Quiroga, S., Kosik, K., and Caceres, A. (2001) *J. Neurosci.* **21,** 2361–2372
18. Shi, S. H., Cheng, T., Jan, L. Y., and Jan, Y. N. (2004) *Curr. Biol.* **14,** 2025–2032
19. Oliva, A. A., Jr., Atkins, C. M., Copenagle, L., and Banker, G. A. (2006) *J. Neurosci.* **26,** 9462–9470
20. Watabe-Uchida, M., John, K. A., Janas, J. A., Newey, S. E., and Van Aelst, L. (2006) *Neuron* **51,** 727–739
21. Bradke, F., and Dotti, C. G. (1999) *Science* **283,** 1931–1934
22. Fukata, Y., Itoh, T. J., Kimura, T., Menager, C., Nishimura, T., Shiromizu, T., Watanabe, H., Inagaki, N., Iwamatsu, A., Hotani, H., and Kaibuchi, K. (2002) *Nat. Cell Biol.* **4,** 583–591
23. Chen, Y. M., Wang, Q. J., Hu, H. S., Yu, P. C., Zhu, J., Drewes, G., Piwnica-Worms, H., and Luo, Z. G. (2006) *Proc. Natl. Acad. Sci. U. S. A.* **103,** 8534–8539
24. Toriyama, M., Shimada, T., Kim, K. B., Mitsuba, M., Nomura, E., Katsuta, K., Sakumura, Y., Roepstorff, P., and Inagaki, N. (2006) *J. Cell Biol.* **175,** 147–157
25. Oguri, T., Takahata, I., Katsuta, K., Nomura, E., Hidaka, M., and Inagaki, N. (2002) *Proteomics* **2,** 666–672
26. Inagaki, N., and Katsuta, K. (2004) *Curr. Proteomics* **1,** 35–39
27. Nomura, E., Katsuta, K., Ueda, T., Toriyama, M., Mori, T., and Inagaki, N. (2004) *J. Mass Spectrom.* **39,** 202–207
28. Niwa, H., Yamamura, K., and Miyazaki, J. (1991) *Gene* (*Amst.*) **108,** 193–199
29. Callebaut, I., de Gunzburg, J., Goud, B., and Mornon, J. P. (2001) *Trends Biochem. Sci.* **26,** 79–83
30. Kukimoto-Niino, M., Takagi, T., Akasaka, R., Murayama, K., Uchikubo-Kamo, T., Terada, T., Inoue, M., Watanabe, S., Tanaka, A., Hayashizaki, Y., Kigawa, T., Shirouzu, M., and Yokoyama, S. (2006) *J. Biol. Chem.* **281,** 31843–31853
31. Yoshimura, T., Arimura, N., Kawano, Y., Kawabata, S., Wang, S., and Kaibuchi, K. (2006) *Biochem. Biophys. Res. Commun.* **340,** 62–68
32. Takagi, H., Somogyi, P., and Smith, A. D. (1984) *J. Neurocytol.* **13,** 239–265
33. Gobel, S. (1975) *Brain Res.* **88,** 333–338
34. Meyer, G. (1982) *Brain Res.* **232,** 455–459

**Supplemental figure 1. Amino acid sequence alignment of human, mouse and rat singar1 and singar2.**

**Supplemental figure 2. Localization of myc-singar1 and myc-singar2 in stage 2 and stage 3 hippocampal neurons.** (A and B) Localization of myc-singar1 (A) and myc-singar2 (B) in stage 2 and stage 3 neurons. Neurons transfected with pCMV-myc-singar1 or pCMV-myc-singar2 were 15 fixed and immunostained by anti-myc antibody. Arrows and arrowheads indicate the axonal and minor process growth cones, respectively. Bars, 50 μm.

## Supplemental Figure 1

```
Human Singar1   1:MSALTPPTDMPTPTTDKITQAAMETIYLCKFRVSMDGEWLCLRELDDISLTPDPEPTH-- 58
Mouse Singar1   1:MSALTPPTDMPTPTTDKITQAAMETIYLCKFRVSMDGEWLCLRELDDISLTPDPEPTH-- 58
Mouse Singar2   1:MSALTPPTDMPTPTTDKITQAAMETIYLCKFRVSMDGEWLCLRELDDISLTPDPEPTHED 60
Rat   Singar1   1:MSALTPPTDMPTPTTDKITQAAMETIYLCKFRVSMDGEWLCLRELDDISLTPDPEPTH-- 58
Rat   Singar2   1:MSALTPPTDMPTPTTDKITQAAMETIYLCKFRVSMDGEWLCLRELDDISLTPDPEPTHED 60

Human Singar1  59:----------------EDPNYLMANERMNLMNMAKLSIKGLIESALNLGRTLDSDYAPLQ 102
Mouse Singar1  59:----------------EDPNYLMANERMNLMNMAKLSIKGLIESALNLGRTLDSDYAPLQ 102
Mouse Singar2  61:SWEDLTDLVEQVRADPEDPNYLMANERMNLMNMAKLSIKGLIESALNLGRTLDSDYAPLQ 120
Rat   Singar1  59:----------------EDPNYLMANERMNLMNMAKLSIKGLIESALNLGRTLDSDYAPLQ 102
Rat   Singar2  61:SWEDLTDLVEQVRADPEDPNYLMANERMNLMNMAKLSIKGLIESALNLGRTLDSDYAPLQ 120

Human Singar1 103:QFFVVMEHCLKHGLKAKKTFLGQNKSFWGPLELVEKLVPEAAEITASVKDLPGLKTPVGR 162
Mouse Singar1 103:QFFVVMEHCLKHGLKAKKTFLGQNKSFWGPLELVEKLVPEAAEITASVKDLPGLKTPVGR 162
Mouse Singar2 121:QFFVVMEHCLKHGLKAKKTFLGQNKSFWGPLELVEKLVPEAAEITASVKDLPGLKTPVGR 180
Rat   Singar1 103:QFFVVMEHCLKHGLKAKKTFLGQNKSFWGPLELVEKLVPEAAEITASVKDLPGLKTPVGR 162
Rat   Singar2 121:QFFVVMEHCLKHGLKAKKTFLGQNKSFWGPLELVEKLVPEAAEITASVKDLPGLKTPVGR 180

Human Singar1 163:GRAWLRLALMQKKLSEYMKALINKKELLSEFYEPNALMMEEEGAIIAGLLVGLNVIDANF 222
Mouse Singar1 163:GRAWLRLALMQKKLSEYMKALINKKELLSEFYEVNALMMEEEGAIIAGLLVGLNVIDANF 222
Mouse Singar2 181:GRAWLRLALMQKKLSEYMKALINKKELLSEFYEVNALMMEEEGAIIAGLLVGLNVIDANF 240
Rat   Singar1 163:GRAWLRLALMQKKLSEYMKALINKKELLSEFYEANALMMEEEGAIIAGLLVGLNVIDANF 222
Rat   Singar2 181:GRAWLRLALMQKKLSEYMKALINKKELLSEFYEANALMMEEEGAIIAGLLVGLNVIDANF 240

Human Singar1 223:CMKGEDLDSQVGVIDFSMYLKDGNSSKGTEGDGQITAILDQKNYVEELNRHLNATVNNLQ 282
Mouse Singar1 223:CMKGEDLDSQVGVIDFSMYLKDGNSSKGSEGDGQITAILDQKNYVEELNRHLNATVNNLQ 282
Mouse Singar2 241:CMKGEDLDSQVGVIDFSMYLKDGNSSKGSEGDGQITAILDQKNYVEELNRHLNATVNNLQ 300
Rat   Singar1 223:CMKGEDLDSQVGVIDFSMYLKDGNSSKGSEGDGQITAILDQKNYVEELNRHLNATVNNLQ 282
Rat   Singar2 241:CMKGEDLDSQVGVIDFSMYLKDGNSSKGSEGDGQITAILDQKNYVEELNRHLNATVNNLQ 300

Human Singar1 283:AKVDALEKSNTKLTEELAVANNRIITLQEEMERVKEESSYILESNRKGPKQDRTAEGQAL 342
Mouse Singar1 283:TKVDLLEKSNTKLTEELAVANNRIITLQEEMERVKEESSYLLESNRKGPKQDRTAEGQAL 342
Mouse Singar2 301:TKVDLLEKSNTKLTEELAVANNRIITLQEEMERVKEESSYLLESNRKGPKQDRTAEGQAL 360
Rat   Singar1 283:AKVDALEKSNTKLTEELAVANNRIITLQEEMERVKEESSYLLESNRKGPKQDRTAEGQAL 342
Rat   Singar2 301:AKVDALEKSNTKLTEELAVANNRIITLQEEMERVKEESSYLLESNRKGPKQDRTAEGQAL 360

Human Singar1 343:SEARKHLKEETQLRLDVEKELEMQISMRQEMELAMKMLEKDVCEKQDALVSLRQQLDDLR 402
Mouse Singar1 343:SEARKHLKEETQLRLDVEKELELQISMRQEMELAMKMLEKDVCEKQDALVSLRQQLDDLR 402
Mouse Singar2 361:SEARKHLKEETQLRLDVEKELELQISMRQEMELAMKMLEKDVCEKQDALVSLRQQLDDLR 420
Rat   Singar1 343:SEARKHLKEETQLRLDVEKELELQISMRQEMELAMKMLEKDVCEKQDALVSLRQQLDDLR 402
Rat   Singar2 361:SEARKHLKEETQLRLDVEKELELQISMRQEMELAMKMLEKDVCEKQDALVSLRQQLDDLR 420

Human Singar1 403:ALKHELAFKLQSSDLGVKQKSELNSRLEEKTNQMAATIKQLEQSEKDLVKQAKTLNSAAN 462
Mouse Singar1 403:ALKHELAFKLQSSDLGVKQKSELNSRLEEKTNQMAATIKQLEQSEKDLVKQAKTLNSAAN 462
Mouse Singar2 421:ALKHELAFKLQSSDLGVKQKSELNSRLEEKTNQMAATIKQLEQSEKDLVKQAKTLNSAAN 480
Rat   Singar1 403:ALKHELAFKLQSSDLGVKQKSELNSRLEEKTNQMAATIKQLEQSEKDLVKQAKTLNSAAN 462
Rat   Singar2 421:ALKHELAFKLQSSDLGVKQKSELNSRLEEKTNQMAATIKQLEQSEKDLVKQAKTLNSAAN 480

Human Singar1 463:KLIPKHH                                                    469
Mouse Singar1 463:KLIPKHH                                                    469
Mouse Singar2 481:KLIPKHH                                                    487
Rat   Singar1 463:KLIPKHH                                                    469
Rat   Singar2 481:KLIPKHH                                                    487
```

**Supplemental Figure 2**

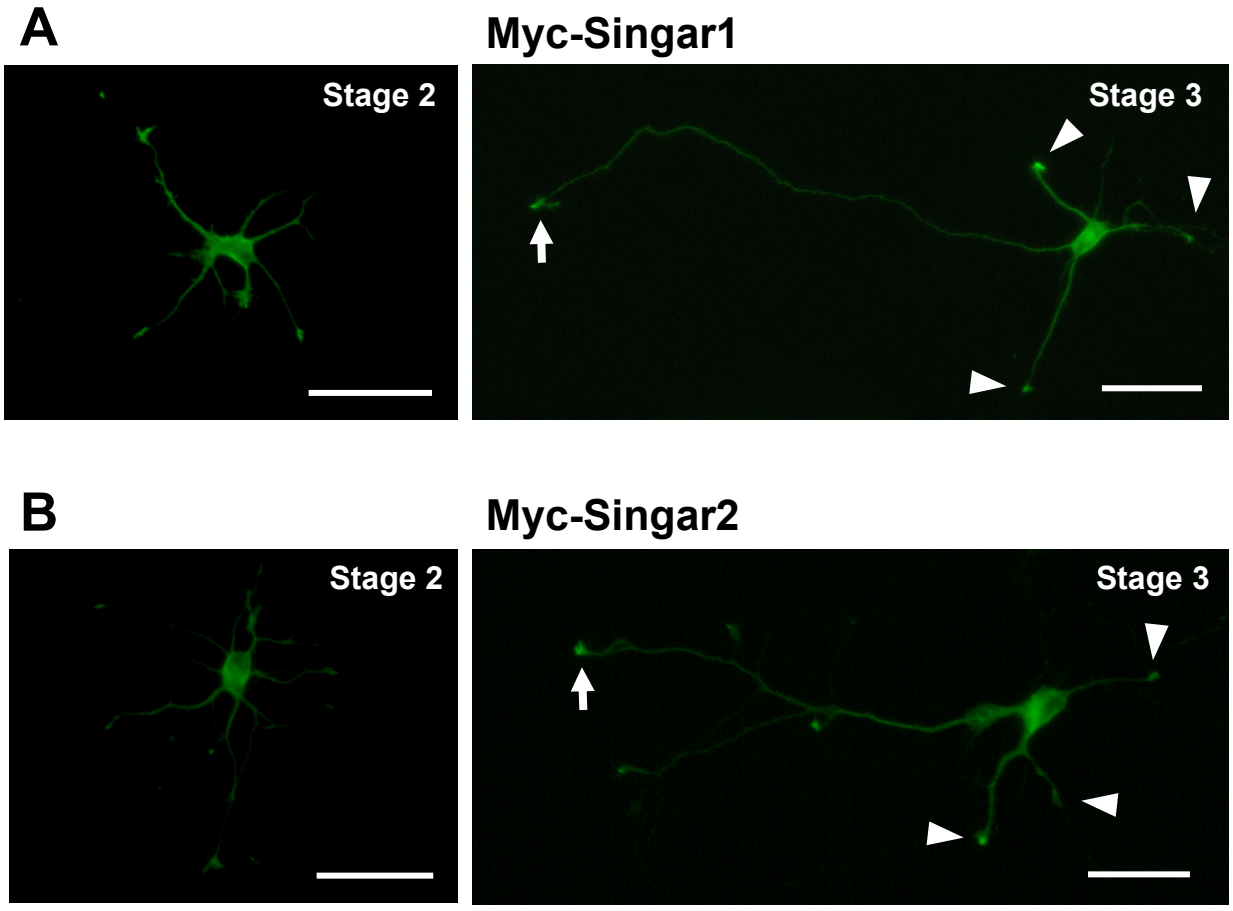

# Singar1, a Novel RUN Domain-containing Protein, Suppresses Formation of Surplus Axons for Neuronal Polarity

Tatsuya Mori, Tomoe Wada, Takahiro Suzuki, Yoshitsugu Kubota and Naoyuki Inagaki

*J. Biol. Chem. 2007, 282:19884-19893.*
*doi: 10.1074/jbc.M700770200 originally published online April 17, 2007*

---